Electronic Supplementary Material (ESI) for Journal of Materials Chemistry A.

Supporting Information

High-performance sodium-ion storage: multi-channel carbon nanofibers free-standing anode contrived via ingenious solvent-induced phase separation

Qingjuan Ren, Zhiqiang Shi*, Lei Yan, Fuming Zhang, Linlin Fan，Lijun Zhang, Wenjie Lv

Tianjin Key Laboratory of Advanced Fibers and Energy Storage, College of Materials Science and Engineering, Tiangong University, Tianjin 300387, PR China

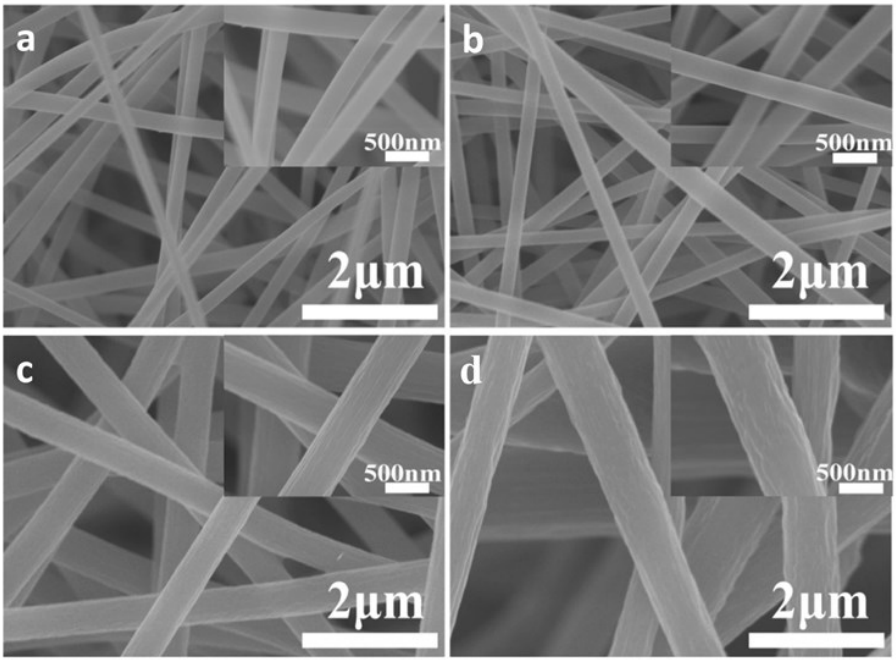

Fig. S1. SEM images of electrospun pristine fibers samples (a) pristine-0 (b) pristine-1 (c) pristine-5 (d) pristine-10.

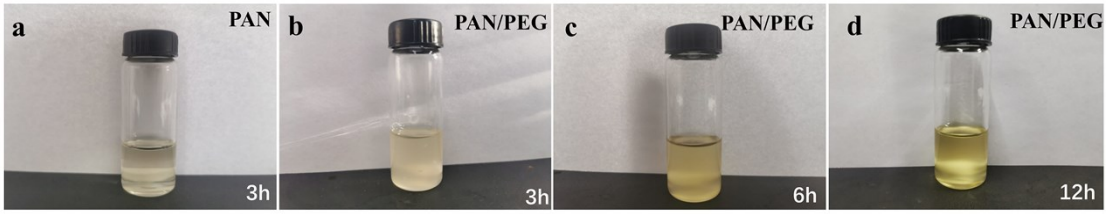

Fig. S2. (a)PAN in DMF at 25 ℃ and the change of solution state after adding 1g PEG (b)3h (c) 6h (d)12h at 60 ℃.

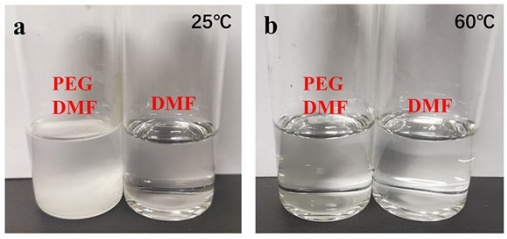

Fig. S3. The state of PEG in DMF solution at different temperatures (a)25℃（b）60℃.

Fig. S4. Tyndall effect. (left)The solution added1g PEG and (right) initial PAN solution.

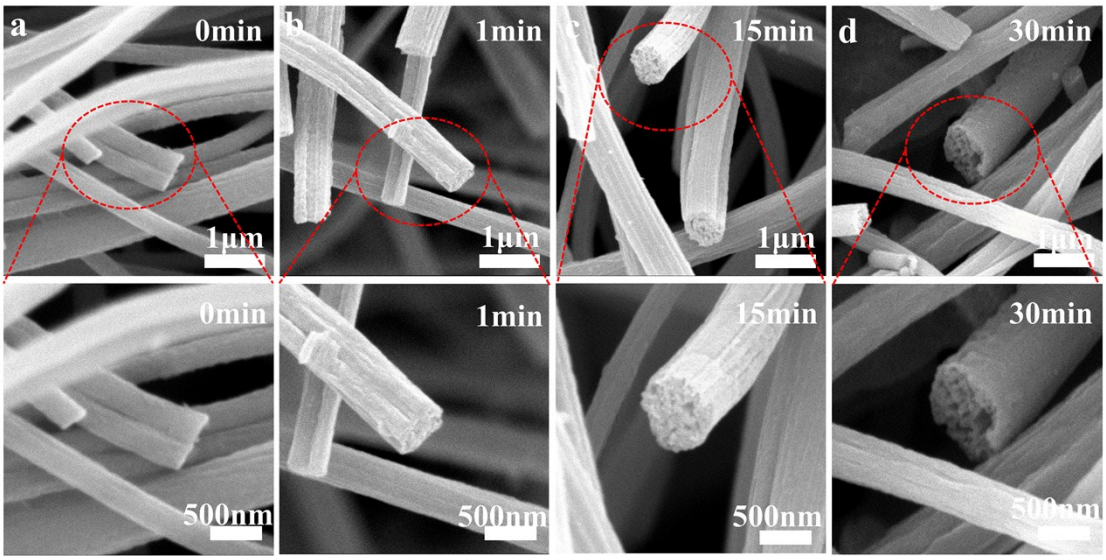

Fig. S5. SEM images of (a)WT-10-0min (b) WT-10-1min (c) WT-10-15min (d) WT-10-30min.

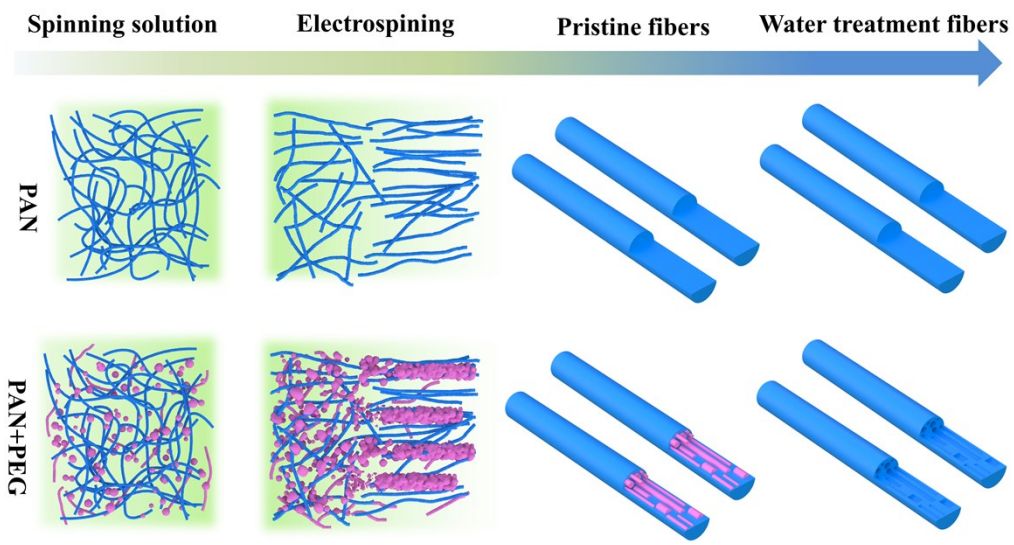

Fig. S6. Mechanism diagram of forming the multi-channel structures.

When PAN is dissolved for 3 hours at 25°C, a uniform and transparent solution can be obtained, and then the solution appears turbid after adding 1g PEG (Fig. S2a-b). Practically, PEG hardly dissolves when added to DMF solution at 25°C, but it dissolves instantly when heated at 60°C (Fig. S3). Interestingly, after heating at 60°C for 3 hours, the spinning solution has turned into a pale yellow liquid but the PEG has not completely dissolved (Fig. S2c). Until continuing to heat for 12 hours, a uniform oily yellow liquid was obtained (Fig. S2d). Due to the oleophobicity of PEG, when more PEG is dissolved in PAN/DMF solution, PEG is more likely to aggregate rather than disperse. Furthermore, there exists more obvious Tyndall effect, when PAN/PEG mixed solution is compared to pure PAN solution (Fig S4).

In the process of electrospinning, the spinning solution undergoes solvent volatilization and orientation stretching of PAN/PEG polymer under a high-voltage electric field, which forms a nanofiber structure. It can be seen that the pristine fiber surface is still smooth (Fig. S5a). However, there are obvious gullies on the fiber surface in the water treatment process only about 1 min and the section of fiber is still solid structures owing to the water non-infiltrated into the fiber (Fig. S5b). With time extends, the fiber cross-section structure has shown obvious channel structure at 15 minutes (Fig. S5c). The PEG is basically completely dissolved for 30 minutes due the water-soluble property (Fig. S5d), which will be further confirmed by TG data later. The detailed mechanism diagram of multi-channel formation is shown in Fig. S6. Partial aggregation

of PEG and orientation stretching of polymer are important conditions for forming channel structure.

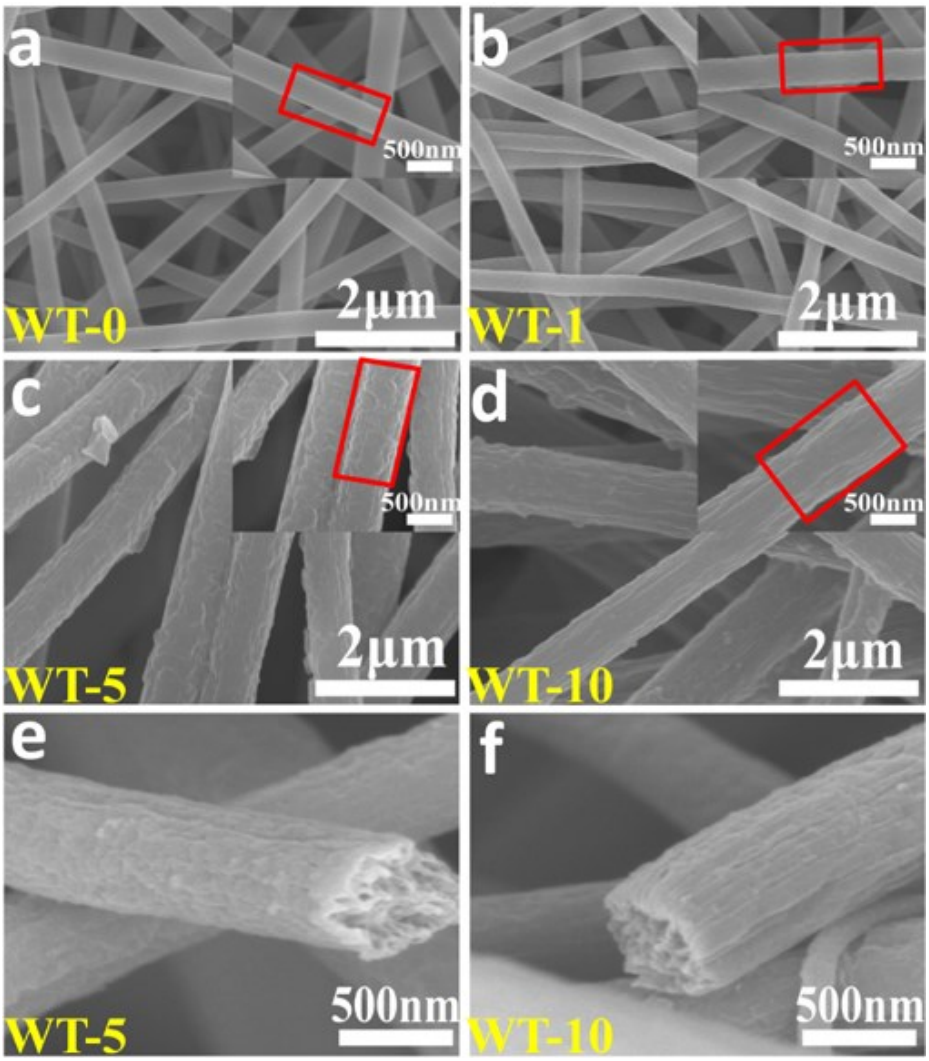

Fig. S7.SEM images of (a)WT-0 (b) WT-1 (c) WT-5 (d) WT-10 and the section SEM images of (e) WT-5 (f) WT-10.

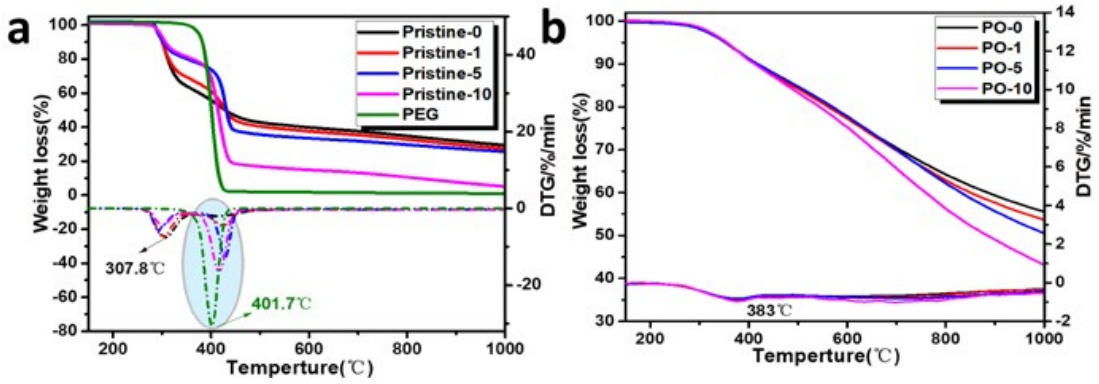

Fig. S8.TG curves of (a)Pristine fibers and（b）Pre-oxidized fibers.

The mysterious effect veil of PEG during the SIPS process was unveiled by TG tests. PEG displays single decomposition temperature ranging from 380 °C to 450 °C, possessing a peak at 401.7 °C (Fig. S8a). With the enhancement of PEG ratio, the mass loss of pristine nanofibers increases in this temperature range. Satisfactorily, the weight loss of four pre-oxidized fibers samples is very close at 383 °C, indicating that PEG has been completely dissolved in the water treatment (Fig. S8b). Moreover, as the amount of PEG added increases, the weight loss of the sample at 600-1000°C increases sequentially, indicating that increased channel structures accelerate the decomposition of the fiber structure during the carbonization process.

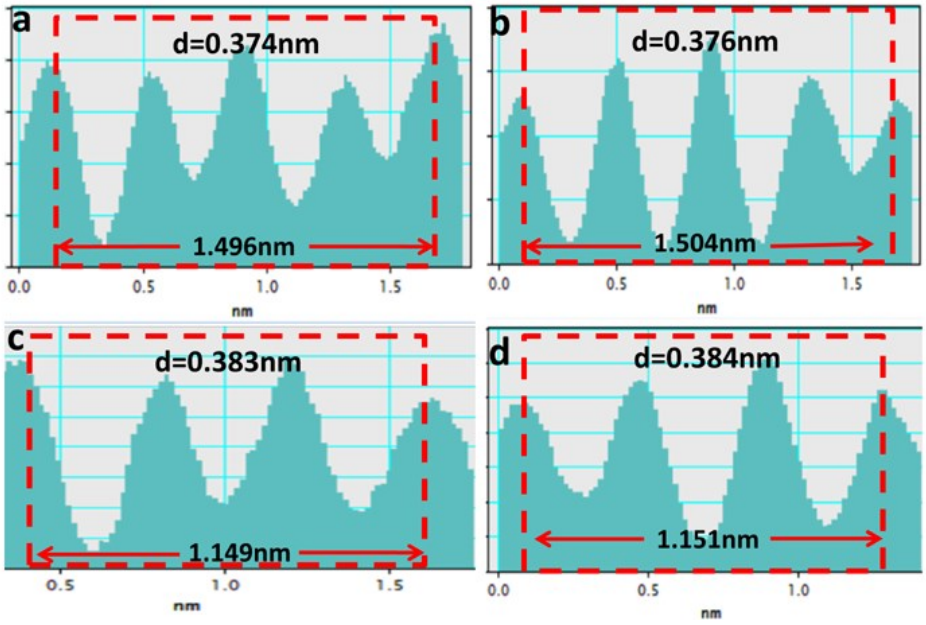

Fig. S9. Measurement of interlayer spacing of different samples in TEM image (a)PCF (b)MCCF-1(c)MCCF-5(d)MCCF-10.

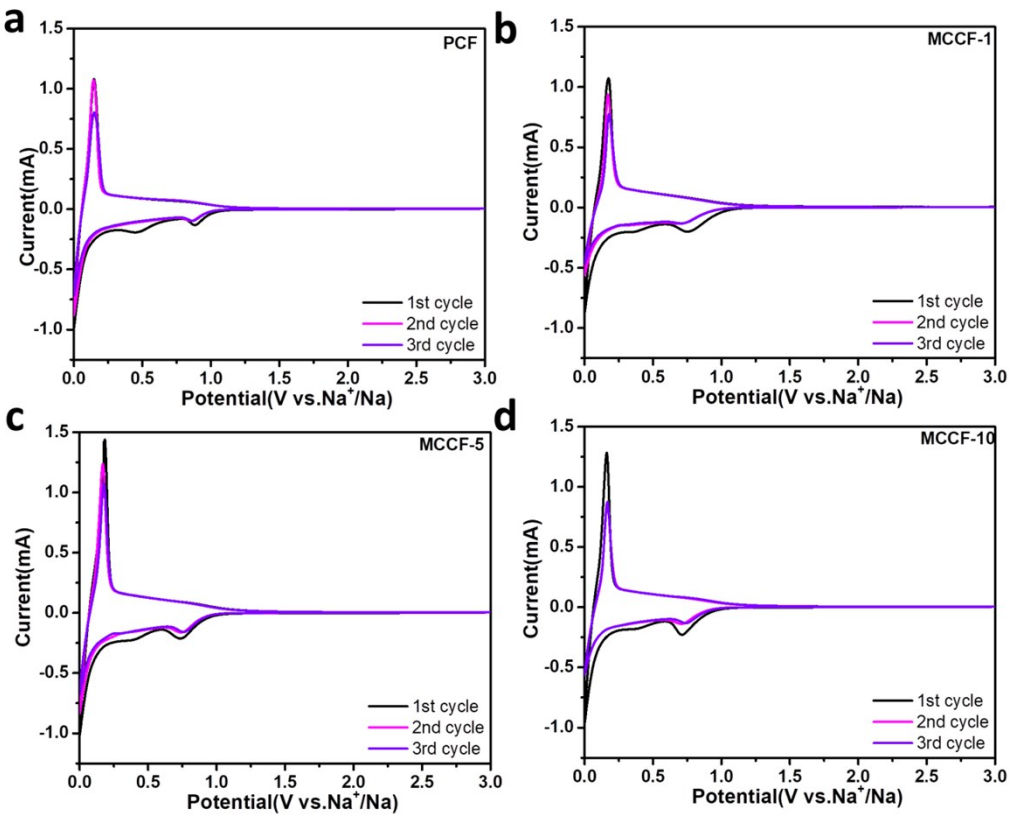

Fig. S10. The first three cycles CV curves for of different samples.

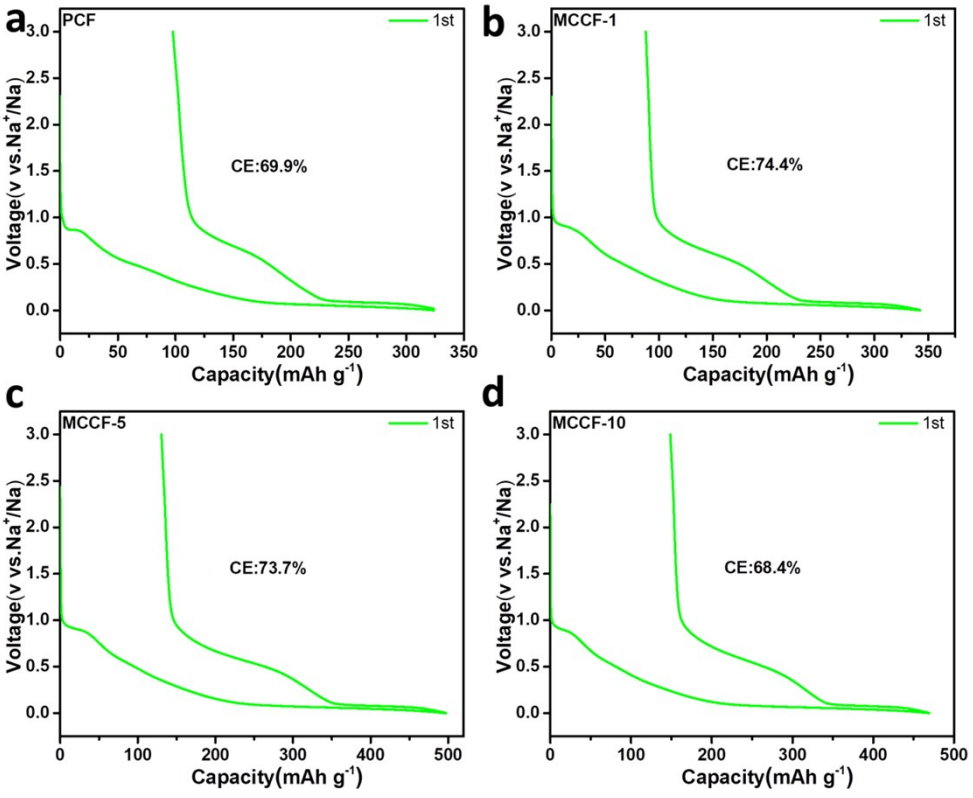

Fig. S11. The 1st GCD profiles of different samples.

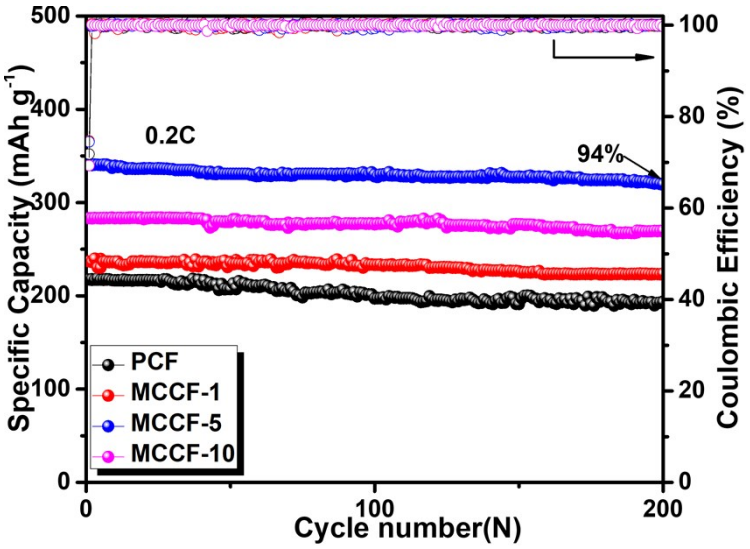

Fig. S12 Cycle stability of samples at 0.2C after 200cycles.

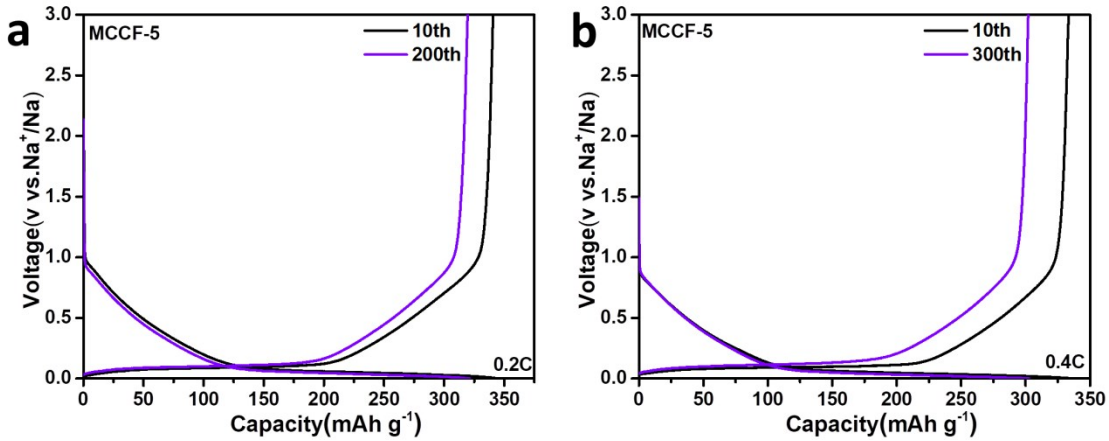

Fig. S13. GCD curves of MCCF-5 samples (a)10th and 200th at 0.2C and (b)10th and 300th at 0.4C.

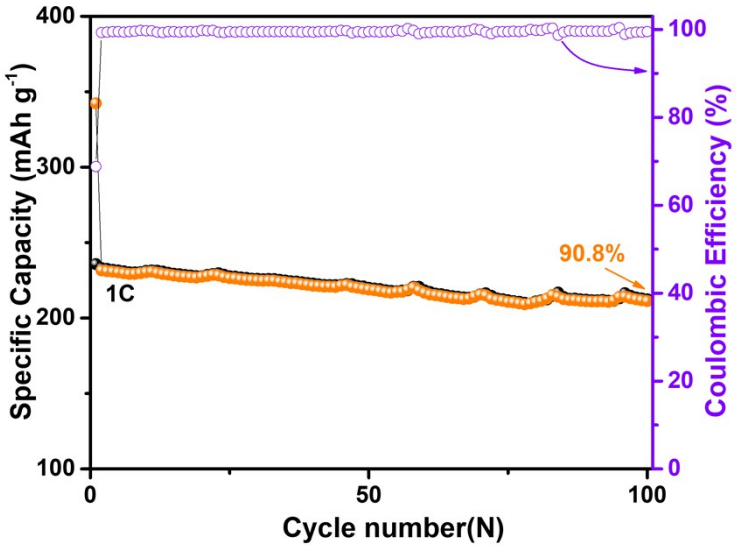

Fig. S14. Cycling performance of the full cell at 1C.

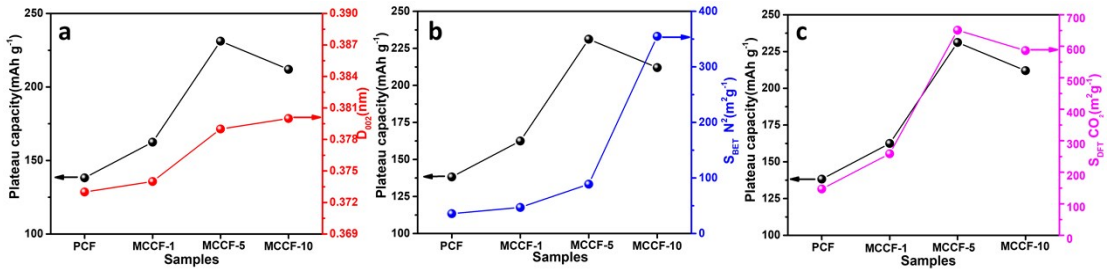

Fig. S15. The varied tendency of (a) plateau capacity and D_{002} (b) plateau capacity and S_{BET} N_2 and (c) plateau capacity and S_{DFT} CO_2.

Table S1. First cycle performance of PCF and MCCFs electrodes.

Samples	1st Discharge capcacity/mAh g^{-1}	1st Reversible capacity/mAh g^{-1}	initial Coulomb efficiency/%
PCF	324.0	226.3	69.9
MCCF-1	342.3	254.6	74.4
MCCF-5	497.0	366.5	73.7
MCCF-10	469.2	320.7	68.4

Table S2. Fit impedance value of different samples.

Samples	Rs/Ω	Rct/Ω	W/Ω
PCF	2.982	118.643	0.002
MCCF-1	2.551	115.765	0.005
MCCF-5	2.432	66.742	0.003
MCCF-10	2.387	60.308	0.002